MDB-5 | 45

MILITARY TECHNICAL COLLEGE
CAIRO - EGYPT

ELASTIC STRESS CONCENTRATIONS IN SIDE-MILLED HOLLOW AND SOLID KEYED CONNECTIONS.

M. H. EISSA *

ABSTRACT

Four, three-dimensional, photoelastic, frozen-stress models of keyed connections were loaded in torsion. This technique was applied to study the axial shear stress distributions in both solid and hollow, side-milled and end-milled keyed connections. The dimensions of the key cross-section were according to the British Inch Standard. The coefficient of friction between the contact surfaces of shaft and hub was measured at the stress-freezing temperature. The surface conditions were arranged to simulate the typical prototype friction. Positions and magnitudes of the peak shear stresses were determined at the different positions of contact between key and shaft keyway. Results from all models are compared and a new key design is described.

* Lecturer, Faculty of Electronic Engineering, Menoufia University, EGYPT.

INTRODUCTION

The analysis of stresses in keyed connections started at the beginning of this century. Gough [1] carried out tests on mild steel shafts with wrought iron keys. He reported that failure occurred at the ends of keys and keyways and the final fatigue crack was always in circumferential direction. He also found a series of cracks radiating from the shaft keyway fillet, showing that the maximum stress concentration occurred there.

Solakian and Karelitz [2] and Gibson and Gilet [3] measured the stresses in keyed connections under torsion, using two-dimensional photoelastic models representing a transverse slice through the keyed assemblies. They observed high stresses at the positions of contact between keyway edges and the key and between the key chamfer and the keyway corners. Peterson [4] observed that the stress field in a keyed connection is three-dimensional and can not be analysed with two-dimensional problems.

Okubo et al [5] used the electroplating technique of strain analysis to measure the shear stresses at the ends of keys and keyway fillets under torsion. They reported that the stresses at the keyway fillet is reduced as the fillet size is increased.

Macdonald [6 to 9] measured the static torsional strength of keyed assembl-ies using different types of steel models. He studied the shear stresses at the contact points between keys and keyways using the photoelastic sandwich technique. He compared the metric [10] and inch [11] standards rectangular, parallel keyed connections. He concluded that the inch connections are slightly better than the metric in static torsion and that the stresses are decreased as the key length is increased.

Orthwein [12&13] applied three-dimensional, photoelastic, frozen-stress technique to determine the tensile stress near the front ends of keys and keyways loaded in torsion. He also studied the effect of key end separation from the keyway end of contact. He suggested a new keyway end shape to reduce the stresses there.

Eissa and Fessler used two-dimensional investigations [14&15] to study the effects of torque magnitude, key width, key thickness, keyway fillet size, hub outside diameter, key chamfer shape, fit of key in shaft, fit of key in hub, fit of shaft in hub and coefficient of friction between components on the elastic stresses in the prismatic part of keyed connections. They applied the photoelastic coating technique [16] to determine the plastic-elastic stress and strain distributions in different steel models. They studied the effects of key length, position of torque reaction, keyway fillet size, imperfect keyway, keyway type and key end shape on the elastic stress distribution using three-dimensional, photoelastic models. They established emperical equations which can predict the elastic stress concentration factors for any key dimension [17 to 21].

In the present work, four, three-dimensional, photoelastic (Araldite), frozen-stress models are used to determine the elastic stress distribution along the key length at the contact lines between keys and keyways, in standard inch keyed connections loaded in torsion with typical coefficient of friction. Solid and hollow, side-milled and end-milled keyed connections

6

are considered. Experimental results are compared with the predicted values from the emperical equations derived by the author before [19].

SHAPES OF THE MODELS

Fig. 1 shows for both types of connections that the hub is as long as the key. The key and keyway dimensions are the standard values for shaft diameter d_o = 4.0 inch [11]. The inner shaft diameter d_i is half the outer one d_o. The main dimensions are:

key width b	key thickness T	keyway fillet radius r
0.256 d_o	0.198 d_o	0.16 d_o

The torque was applied to the hub through two diametrically opposite pins as shown in Figs. 1 & 2.

The fits between the components were:

a. interference of key in shaft keyway
b. transition of key in hub keyway
c. transition of shaft in hub

The minimum material conditions were used during manufacturing the models to study the worst case of the connections. The measured coefficient of friction varied between 0.14 and 0.15 with silicone greased contact surfaces.

EXPERIMENTAL WORK

Models were machined from castings of Araldite CT 200 with Hardener HT 907 (mixture 100: 60; parts by weight). Shafts and hub bores were ground to surface finish CLA values between 2 and 4 μm. The roundness was also measured for all models; the maximum out-of-roundness was about 4 μm.

The keyway profile produced by the specially ground cutters were checked before the cutters were used. Key sides were ground to ensure the correct fits in keyways. Maximum parallelism error between the keyway and the shaft axis was about 15 μm.

The models were loaded in pairs as shown in Fig. 2 with the middle of the keys in the same horizontal plane as the shaft axis, immersed in dense, inert oil to minimise self-weight effects. The torque was applied to the hubs through the two diametrically opposite pins shown in Figs. 1 and 2. The hubs rested in Vee-blocks but the remainder of the front hub weight was counterbalanced to eliminate any frictional restraint there as reported before [18].

After the stress-freezing cycle was applied, keys were glued to the shaft (at the keyway free side) and sliced together perpendicular to the keyway surface. Main slices were 1.5 mm thick in the prismatic part and 1.0mm thick in the keyway ends. Sub-slices cut from the main slices, needed to determine the principal stress directions were 0.5 mm thick.

6

ANALYSIS

All stresses were determined from photoelastic, normal incidence readings. Oblique incidence measurements would subject to large errors due to large stress gradients associated with the small fillet radii and contact conditions.

Nominal stresses were determined from slices cut at 45° to the shaft axes in the plain, central parts. The calculated probable errors of stress index were:

a. typical probable error is 4 %
b. greatest probable error is 7.5 %

Co-ordinate directions were defined as shown in Fig. 1 and 3. The contact stress perpendicular to the keyway surface, in the y direction was called σ_c . It was always a principal stress along the key length. The stress least inclined to the x direction is approximately axial in the prismatic part was called σ_a . The third principal stress was called σ_t . All are shown in Fig. 3 for a point in the keyway end.

The maximum shear stresses at all positions of contact were determined from the following two equations [17]. By viewing the main slice and sub-slice normally we get:

If $\sigma_a > \sigma_t > \sigma_c$

$$\sigma_a - \sigma_c = F \left(n_x / t_x + n_y / t_y \cos^2 \alpha \right) \qquad (1)$$

If $\sigma_t > \sigma_a > \sigma_c$

$$\sigma_t - \sigma_c = F \left(n_x / t_x + n_y / t_y \sin^2 \alpha \right) \qquad (2)$$

Where F is the material fringe value. The relative values of the principal stresses were determined using a wedge compensator. Because large stresses occur in keyed connections, the local maximum shear stress is a good indication of the severity of the stressing at a point.

RESULTS AND DISCUSSION

Large stresses only occur where the transmitted torque is concentrated due to the discontinuities of key and keyway profiles [18] . The greatest stresses were always in the surfaces of contact between key and keyways. Results are only presented for the three contact lines between key and shaft keyway, i.e. Sb, Ss, Se and at key hub contact line Kh.

Figure 4 shows the stress distributions along the prismatic part and around the keyway ends as calculated from equations 1&2, i.e. either $\frac{1}{2} (\sigma_a - \sigma_c)$ or $\frac{1}{2} (\sigma_t - \sigma_c)$.

Common Features of Results From all Models

All contact stresses in most of the prismatic parts of all models decrease approximately linearly away from the keyway end. The maximum values are always at or near the front where most of the torque is transmitted [18].

6

In the keyway ends the stresses are always minimum and increase to a max: in the prismatic part at the end of the side-milled connectioms and at the shaft bottom Sb (in end-milled connections) or to a maximum in the round end and another maximum in the prismatic part at the other contact lines (Ss & Se) in end-milled connections only.

Table 1 shows the maximum values of I for the different positions of contact in both the prismatic part and the round end of shaft keyway and key for all models. Table 1 shows the following common features:

a. the contact stress at Sb is never the greatest in the shaft keyway
b. in the shaft keyway the greatest stress in the prismatic part occurs at Ss
c. in the key the greatest stress occur at Kh in the end-milled connections and at Ks in the side-milled ones.

Table 1. Maximum stress indices at shaft and key contact lines.

model ref.	keyway type	x_p / d_o	prismatic part				end	
			Sb	Ss	Se	Kh	Ss	Se
1 m	end-milled	.04	3.3	3.6	3.4	5.4	3.65	5.2
2 m	,,	.01	3.5	3.7	3.6	5.5	0.95	1.1
3 m	side-milled	.0	4.2	5.3	5.5	4.5	----	----
4 m	,,	.00	4.9	6.4	6.2	4.8	----	----
5 m	end-milled	.04	3.2	3.3	3.2	5.3	4.4	4.6
6 m	side-milled	0.0	3.6	4.0	3.4	4.5	----	----

The following should be noticed in Table 1:

1. model 4 m has a hollow shaft with $d_i = \frac{1}{2} d_o$
2. all coefficients of friction were 0.15
3. maximum stress at Kh for model 2 m occurs at $x_p / d_o = .02$
4. key of model 2 m is chamfered and rounded, while that of model 6 m is rounded.
5. results of model 5 m are predicted from the equations derived by the author before [19].
6. model 6m is suggested by the author to reduce contact stresses at the front of the connection.

Comparison Between End-milled and Side-milled Connections

From Figure 4 , it can be seen that in most of the prismatic parts of both models the stresses are similar. At $x_p / d_o = 0.0$ in the side-milled connections, the stresses are increased due to the contact between the sharp edges of the key end and keyway surfaces. It might be expected that these stresses would be reduced if those sharp edges are rounded using a file as shown in Fig. 1. Comparison between the results of the suggested model "6 m" and model "1 m", shows that the decrease in the maximum stresses at Se is about 34 % and at Kh is about 26 %. The increase at Ss is about 9.5 % and at Sb is about 8 % . The latter is very near to the experimental errors.

Comparison Between Solid and Hollow Side-milled Connections

Comparison between models 3 m & 4 m is given below:

position	Sb	Ss	Se	Kh
$\frac{I_3}{I_4}$	0.86	0.83	0.89	0.95

It is clear that the stresses at contact lines in the shaft are well affected by this drastic reduction in the radial thickness near the keyway bottom, as it was 0.42 d_o in the solid model and has become 0.17 d_o in the hollow one. Of course this reduction increased keyway distortion in the shaft resulting the above increases as shown in Table 1. The increase in stresses varied between 12 & 20 % in the shaft contact lines, while at Kh the increase is within the experimental errors.

Finally, the predicted values of the maximum stresses [19] show good agreement with the experimental results in particular at the contact positions in the prismatic part.

CONCLUSIONS

Stress distributions in keyed connections are very complicated due to the discontinuities of profiles of keys and keyways surfaces at the multiple contact and the different loading modes they are usually subject to.

The following can be concluded:

1. Stresses could be reduced in end-milled connections by using chamfered and rounded key ends.

2. Stresses in side-milled connections could be reduced if rounded key ends are used.

3. Stresses in hollow shaft keyway are greater than those of the solid one. It might be expected that a shaft with $d_i = d_o/4$, will not affect the local stresses at the shaft contact lines.

4. A chamfered and rounded end-milled keyed connection is the optimum connection as it has the lowest stress concentrations and the smaller keyway length compared to the suggested side-milled connections.

6

ACKNOWLEDGEMENTS

The author would like to thank the NOTTINGHAM UNIVERSITY technicians for their skilled assistance in casting and slicing the models and the Depart--ment of Mechanical Engineering for providing the necessary facilities.

REFERENCES

1. Gough, H.J. " The Effect of Keyways Upon The Stiffness of Shafts Subjected to Torsional Stresses" Aeron. Research Council, Tech. Report 488(1925).
2. Solakian, A.G. and Karelitz, G.B. " Photoelastic Study of Shearing Stresses in Keys And Keyways" Tr. ASME, 54 (1932).
3. Gibson, W.H.H. and Gilet, P.M. " Transmission of Torque by Keys And Keyways" Jr. Instn. Eng., Australia, 10 (1938).
4. Peterson, R.E. " Fatigue of Shafts Having Keyways" Proc. ASTM, 32 (21),(1932).
5. Okubo,H., Hosono, K. and Sakaki, K." The Stress Concentration in Keyways When Torque is Transmitted Through Keys" Exp. Mech., 8(1968).
6. Macdonald, D.M."Static Torsion Tests on Shrink-fits and Keyed Conne--ctions" NEL Report, Glasgow, U.K., 489 (1971).
7. Macdonald, D.M. "Comparison of Inch And Metric Keys in Static Torsion" NEL Report, Glasgow, U.K. ,526 (1972).
8. Macdonald, D.M." Loaded Key Reaction And Stresses" NEL Report, Glasgow, U.K., 606 (1976).
9. Macdonald, D.M. "Key Length And It's Effect on The Static Torsional Strength of Keyed Joints" NEL Report, Glasgow, U.K., 635 (1977).
10. British Standard Institution: Metric Keys And Keyways BS 4235, Part I (1967).
11. British Standard Institution: Inch Keys And Keyways. BS 46, Part I, (1958).
12. Orthwein, W.C. "Keyway Stresses When Torsional Loading is Applied by The Keys" Exp. Mech., 15 (1975).
13. Orthwein, W.C. " A New Key And Keyway Design" Trans. ASME, J Mech. Design, 101 (1979).
14. Eissa, M. and Fessler, H. " Elastic Stresses Due to Torque Transmi--tted Through The Prismatic Part of Keyed Connections" Part I "Standard Shapes With Different Fits And Friction" J. St. Ans.,17 (2),(1982).
15. Eissa, M. and Fessler, H. "Elastic Stresses Due to Torque Transmitted Through The Prismatic Part of Keyed Connections" Part II,"Effect of Shape With Usual Fits And Friction" J. St. Ans., 17(4), (1982).
16. Eissa, M. and Fessler, H. " The Photoelastic Coating Technique For Plastic-Elastic Contact" Exp. Mech., September (1983).
17. Eissa, M. and Fessler ,H. "Reduction of Elastic Stress Concentration in End-milled Keyed Connections" SESA Spring Meeting, Dearborn,(1981).
18. Eissa,M. and Fessler, H. "Distribution of Transmitted Torque And Elastic Stresses in Keyed Connections" 7th Intr. Conf. Exp. Str. Ans, Haifa , Israel, Aug.(1982).
19. Eissa, M. "Elastic Stress Distribution in Solid and Hollow End-milled Keyed Shafts" PEDAC, ALEXANDRIA, Dec. (1983).
20. Eissa,M. and Fessler, H." Three-Dimensional Elastic Stress Distrib--ution in End-milled Keyed Connections" J.Str. Ans. , 18 (2), (1983).
21. Eissa,M. and Fessler, H." Photoelastic Stress Distributions in End-milled And Side-milled Keyed Connections Under Torsion" AMSE (1983)

NOTATION

Dimensions and positions of contact are defined in Fig. 1.

I	stress index, $(n_x/t)/(n_{nom}/t_{nom})$.
n_x , n_y	fringe orders in x and y directions
t_x , t_y	slice thicknesses defined in Fig. 3.
x_p	position in prismatic part (see Fig. 1.)
x, y, z, Ø	co-ordinate directions defined in Fig. 3.
σ_c , σ_t , σ_a	principal stresses as shown in Fig. 3.

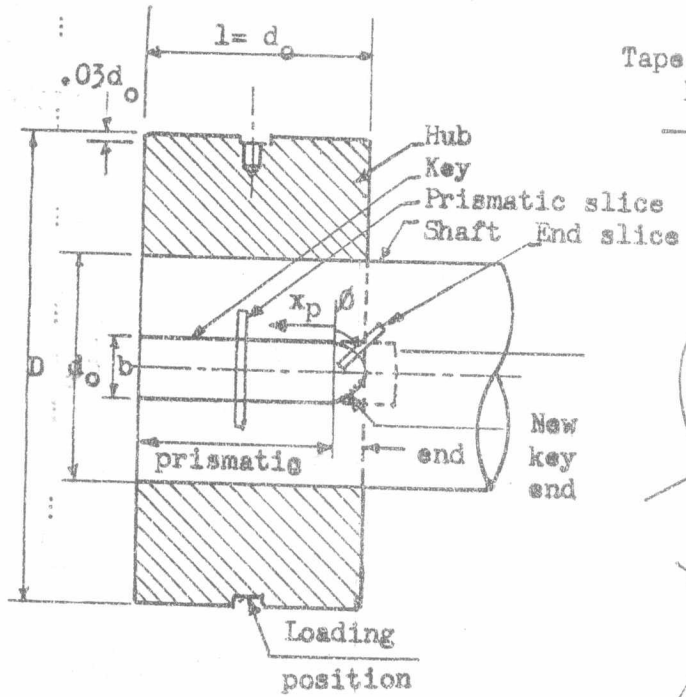

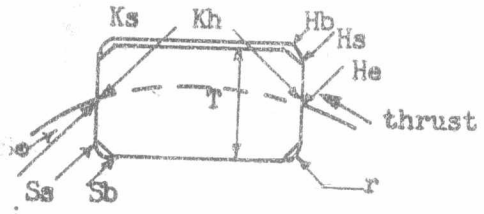

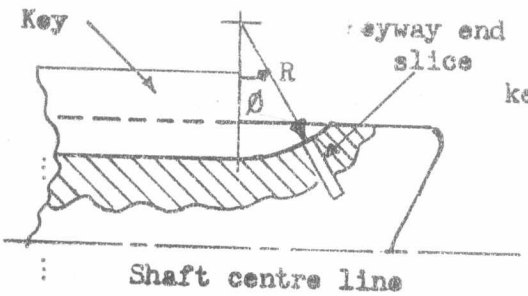

Fig. 1. Model dimensions.

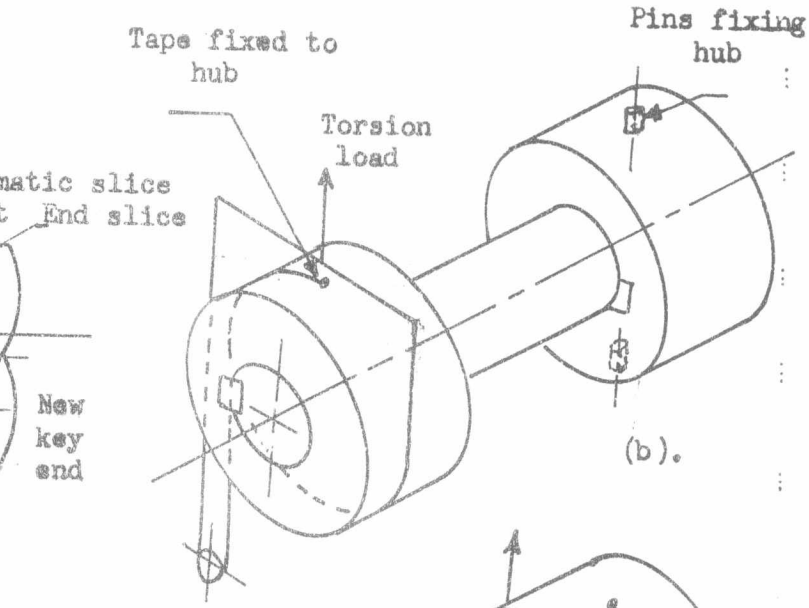

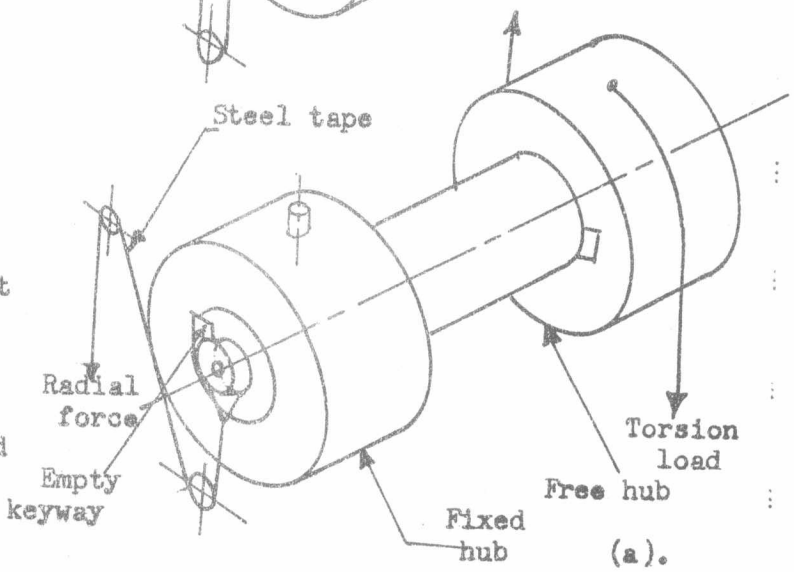

Fig. 2. Torque and friction arrangements.

6

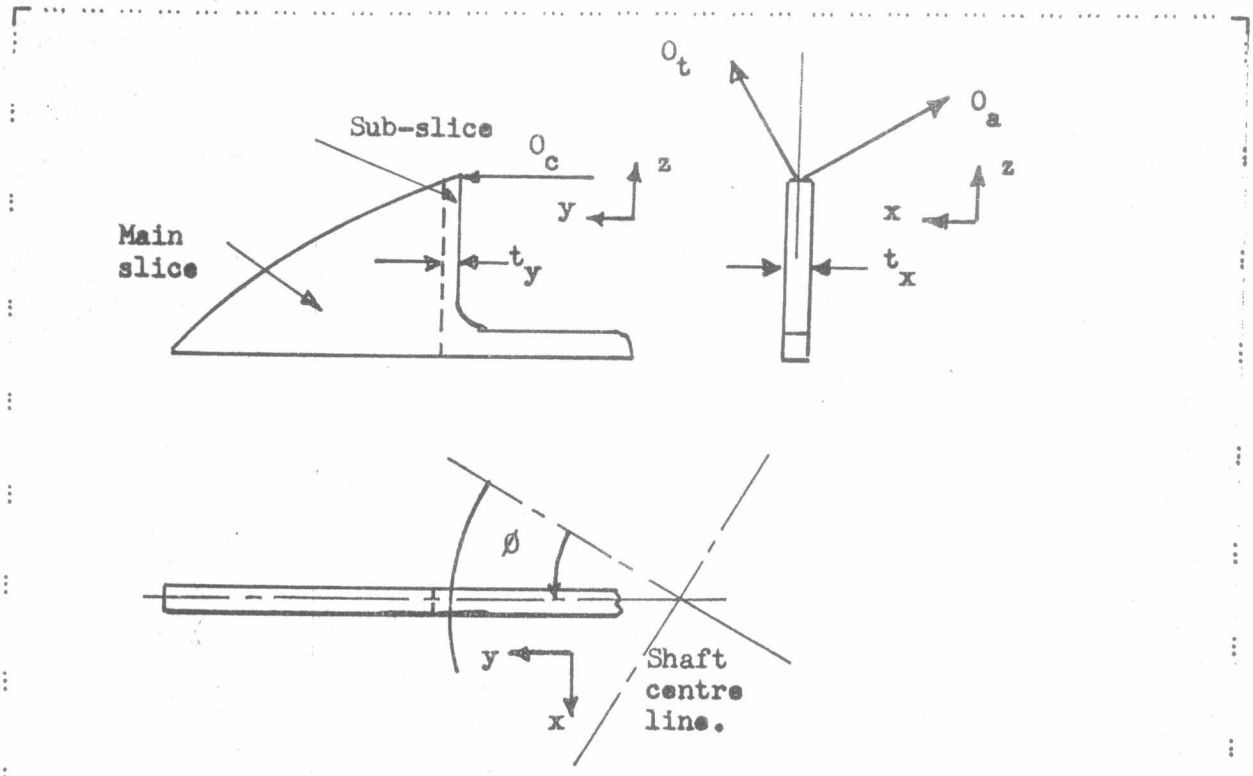

Fig. 3. Co-ordinates and directions of the principal stresses at a point in the keyway end.

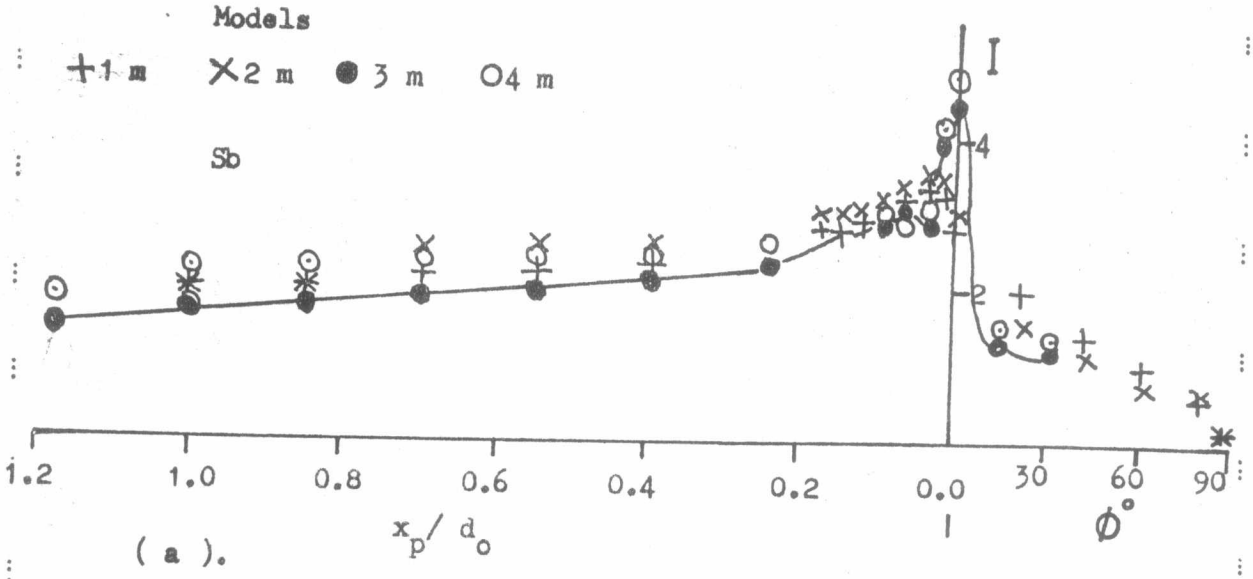

Fig. 4 (a). Stress distribution at Sb.

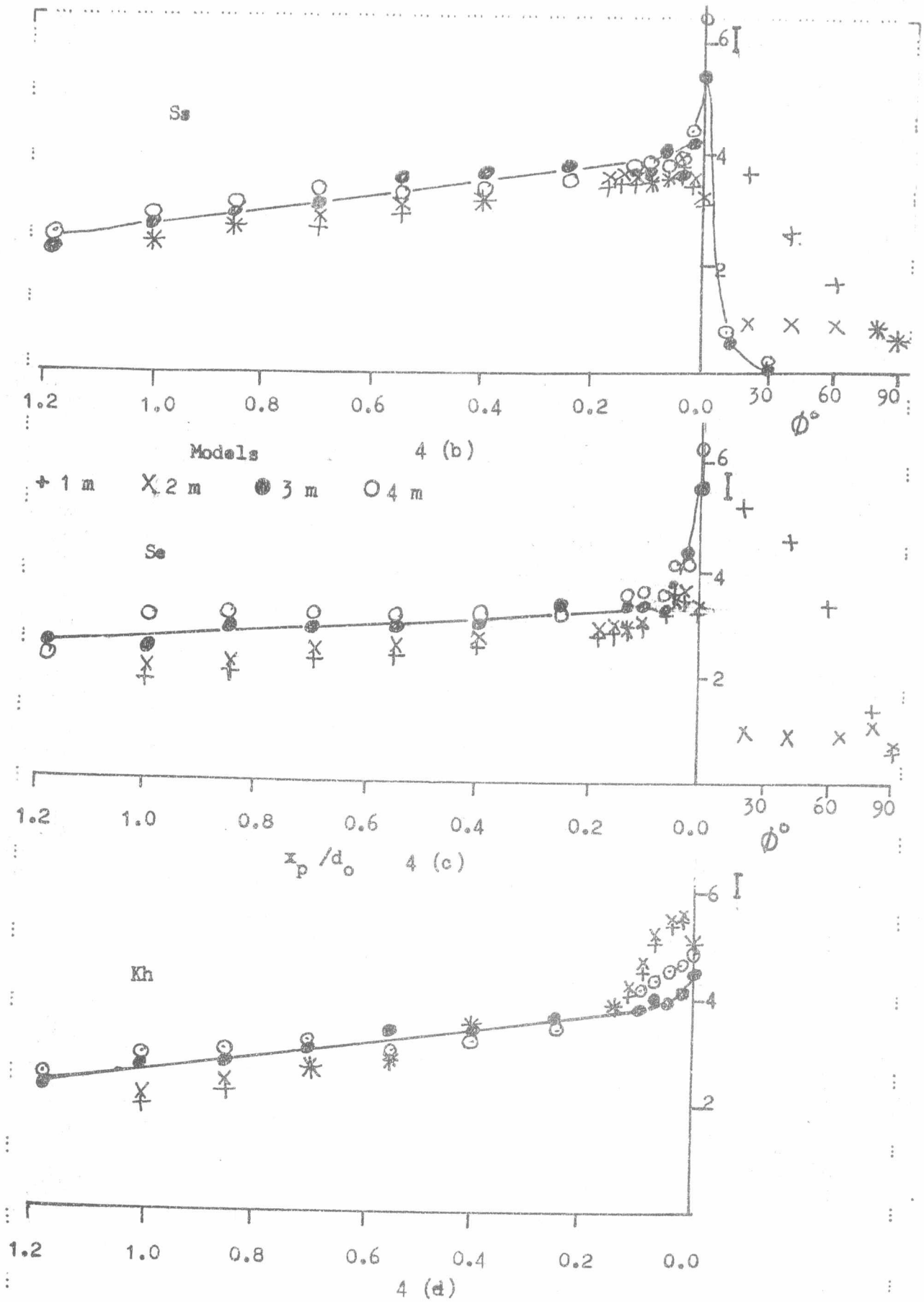

Fig. 4 (cont.) . Stress distributions at Ss, Se &Kh.